Power Consumption and Radiation Trade-offs in Phased Arrays for 5G Wireless Transport

Steven Caicedo Mejillones*†, Matteo Oldoni*, Stefano Moscato*, Alessandro Fonte* and Michele D'Amico†

*R&D Department, SIAE Microelettronica, Cologno Monzese, Italy

†DEIB Department, Politecnico di Milano, Milan, Italy

Email: [steven.caicedo, matteo.oldoni, stefano.moscato, alessandro.fonte]@siaemic.com, [michele.damico]@polimi.it

Abstract—**5G access network targets mmWave frequencies for Enhanced Mobile Broadband scenarios. This in turn leads to densification of the base stations to overcome the high propagation losses of mmWaves. Furthermore, 5G fronthaul/backhaul network is expected to be fiber optic based. However, a fully optical network is not feasible in hyper dense scenarios, mainly because of the cost it represents. This leaves enough space for point-to-point wireless links. Stepping forward, new wireless backhaul network is expected to be reconfigurable to satisfy the dynamic nature of the mobile traffic. Phased Array Antenna (PAA) on backhaul equipment is a promising solution to answer this need. However, there are challenges to overcome before using it in a commercial equipment, power consumption is one of them and this paper tries to summarize possible solutions to minimize it, providing that the total system gain of the current equipment is preserved and the regulatory radiation masks are fulfilled.**

Keywords—**backhaul; mmWave; phased array antenna; power consumption; radiation masks; transport network; 5G.**

I. INTRODUCTION

The current backhaul network is static, meaning it connects prescribed pairs of sites, and therefore it is not possible to recover from a link failure caused by link misalignment or a change in the propagation environment, nor can it be reconfigured to efficiently meet the dynamic demands of mobile traffic. These issues can be overcome by using PAAs that provide capabilities of beam steering to the equipment and reconfiguration to the network.

On the other hand, the current backhaul links are designed to satisfy a multi-Gbps traffic often with an availability of more than 99.995%. Taking into account the high losses of the mmWave propagation (frequencies also used in backhaul), it requires the antennas currently used to be highly directive. This implies that the current total System Gain (SG) is very high. The new PAA must also meet this high SG. This in turn could result in a high energy consumption.

Within the literature, a lot has been published on PAA but mainly related to antenna architecture and overall performance [1][2]. Moreover, a lot of effort has been spent to reduce the antenna size and make it low-profile and lightweight [3][4]. Some other references point out the cost as the main driving feature in PAA design and development [5][6]. On the contrary, very few publications on antenna array focus

the attention on the power consumption mainly because the passive antenna topic is often unrelated to the active parts (i.e. MMICs). Within the practical deployment of PAAs, their power consumption is a clear limitation because it affects the thermal and mechanical design complexity of the overall structure. This imposes severe constraints on power supply and raises the operating expenses (OpEx) which are an important figure from the final user point of view (telecom operators).

This paper tries therefore to summarize the possible solutions to minimize the power consumption keeping into account that the SG must be preserved and the Radiation Pattern Envelope (RPE) requirements of ETSI and similar regulatory bodies have to be fulfilled. The beam steering capabilities are shown for each case.

To perform the study, first the single antenna element is designed and simulated. The base elements considered in this study are: a patch antenna, a sub array of patch antennas and a horn antenna. Then the array size is calculated considering the gain of the base element, the SG required and the output power of each power amplifier (PA). As final step, the corresponding power consumption is computed. The optimum output power of the PA that minimizes the power consumption in PAAs was analytically calculated. Finally, the array is simulated, obtaining the radiation pattern at different steering angles.

The next sections of the paper are organized therefore as follows. Sections II and III describe the objectives and the power consumption model followed. Sections IV and V present the results and discussions. Finally, section VI summarizes the conclusions.

II. REQUIREMENTS

The final target is to replace the current reflector antenna used by the 26 GHz commercial backhaul equipment manufactured by SIAE Microelettronica for a PAA. Therefore, the new PAA is constrained by the following: the equipment uses FDD duplexing, the antenna radiation pattern must satisfy at least the RPE class 2 of ETSI [7], the SG defined by

$$SG = P_{\text{tx}} \times G_{\text{tx}} \times G_{\text{rx}} \ , \tag{1}$$

has to be maintained after the replacement. The current equipment at 26 GHz has an output power of $P_{\text{tx}} = 30\text{dBm@P1dB}$, the gain of the reflector antenna is $G_{\text{tx}} = G_{\text{rx}} = 36$ dBi (tx is transmission and rx is reception). Thus, the PAA must

provide 102 dBm of SG, which would allow to preserve current hop-lengths and availabilities. Beam steering of at least $\pm30°$ is expected on both elevation and azimuth planes. Power consumption should be kept as low as possible, considering 100 W as the current power consumption of the equipment.

III. POWER CONSUMPTION MODEL

The PAA architecture consists of N active components connected to M antennas. Each active component has two phase shifters (PS), one connected to a PA in the transmission chain, the other to a low noise amplifier (LNA) in the reception chain. Adjusting (1) to the PAA architecture, we have:

$$SG = (P_{\text{tx}} \times N) \times (G \times M)^2 \quad , \quad (2)$$

where P_{tx} is the output power of each of N PAs and G is the gain of each of M antennas. Note that the antenna here is generic, and may be a patch, a horn, etc. Considering that $M = k \times N$, where k is the number of antennas that are grouped and handled by one active element, therefore:

$$SG = P_{\text{tx}} \times G^2 \times k^2 \times N^3. \quad (3)$$

On the other hand, the DC power consumption of N active components is estimated by [8]:

$$P_{\text{DC}} = N \times \left(\frac{P_{\text{tx}}}{\eta_{\text{PA}}} + P_{\text{TxOH}} + P_{\text{LNA}} + P_{\text{RxOH}} \right) \quad , \quad (4)$$

where η_{PA} is the drain efficiency of the PAs. P_{LNA}, P_{TxOH} and P_{RxOH} are the power consumption of the LNAs, and of the overhead components (e.g. PS) respectively. Then, merging (3) and (4) we have $P_{\text{DC}}(N)$:

$$P_{\text{DC}}(N) = \frac{SG}{N^2 \times (kG)^2 \times \eta_{\text{PA}}} + \quad (5)$$
$$N \times (P_{\text{TxOH}} + P_{\text{LNA}} + P_{\text{RxOH}}) \quad .$$

Minimizing this equation ($\frac{\text{d}P_{\text{DC}}(N)}{\text{d}N} = 0$), N_{OP} is given by:

$$N_{\text{OP}} = \sqrt[3]{\frac{3 \times SG}{(kG)^2 \times \eta_{\text{PA}} \times (P_{\text{TxOH}} + P_{\text{LNA}} + P_{\text{RxOH}})}} \quad . \quad (6)$$

Finally replacing N_{OP} in (4) and (5), the optimum P_{TxOP} and the minimum P_{DCmin} are respectively [8] [9]:

$$\frac{P_{\text{TxOP}}}{\eta_{\text{PA}}} = \frac{P_{\text{TxOH}} + P_{\text{LNA}} + P_{\text{RxOH}}}{2} \quad , \quad (7)$$

$$P_{\text{DCmin}} = \frac{3}{\eta_{\text{PA}}} \times \sqrt[3]{\frac{SG \times P_{\text{TxOP}}^2}{(kG)^2}} \quad . \quad (8)$$

It appears obvious before any mathematical dissertation that the minimization of the overall power consumption is directly proportional the main PA power efficiency. Although commercial components may not be the state-of-the art, literature about Monolithic Microwave Integrated Circuits (MMICs) shows that efficiency of basic components has not dramatically increased. The high frequency involved together with the linearity demanded by the actual modulation standards (up to 4096 QAM) lead to the forced choice of GaAs-based

MMIC. The upcoming SiGe-based technology is not fully established for the mm-wave spectrum and the delivered output power is still not sufficient to cover actual needs. The last high-power upcoming technology is clearly GaN-based where the semiconductor structure allows drain voltages up to 48V with higher output impedance, lower losses due to matching networks and wider bandwidth. This last promising technology is already adopted within wireless backhauling across lower frequencies but in the next years the progressive shrinking of MMIC technology promises its adoption also into mm-wave bands.

Back to the equations, it can be noticed that for a given SG there are several ways to reduce the power consumption: devising a PA with an ad-hoc output power P_{TxOP}, increasing the gain G of the base element, or using subarrays ($k >= 1$). Increasing the efficiency of the PA is out the scope of this work and it is assumed 15%, a reasonable value for industrial-level PAs. Therefore, three cases were analyzed:

1) A PA with an ad-hoc output power P_{TxOP} is considered. The curves N, P_{DC} vs P_{Tx} were computed to confirm the optimum equations. The base element was a patch antenna, of size 4.6×3.5 mm^2 respectively, using the substrate RT/duroid$^®$ 5880 (ϵ_{r}=2.2, h=0.508 mm), the simulated gain G was around 6 dBi. The values of P_{LNA}, P_{TxOH}, P_{RxOH} are 340 mW, 10 mW, 10 mW respectively according to SIAE's devices.

2) The same of the previous case with the difference that the base element is a 2x2 subarray ($k = 4$) of patch antennas previously mentioned. For this case a decrease of beam steering performance is expected, because there is no phase control over every element. The sub-array approach also leads to extra losses due to the longer feeding network, which mainly depends on the adopted technology. However, considering the case of a simple microstrip splitting network, the efficiency penalty is in the order of few tenths of dB.

3) Similar to case 1, but using, as base element, a horn antenna with flare height, width, length of $12 \times 12 \times 12$ mm^3 and the waveguide size of $5 \times 10 \times 12$ mm^3 respectively . The simulated gain was 10 dBi approximately. If on one hand the advantages in terms of gain are evident when adopting such radiator, the penalty to be paid relies in the manufacturing cost, size and weight but also in the limited scanning capabilities due to grating lobes.

IV. RESULTS

Analyzing the curves of the Fig. 1 a and b, computed by using (3) and (4) respectively in conjunction with the assumptions written in the caption of the figure, it can be realized that the minimum power consumption for the three cases 1, 2, and 3 are 180 W, 78 W, and 97 W respectively, which matches perfectly with the values computed with (8). It is important to note that P_{TxOP} = 15 dBm is the same for all three curves, it means it is independent on the gain G of the base element even if a subarray is used. This was predicted by (7), since P_{TxOP} only depends on η_{PA}, P_{LNA},
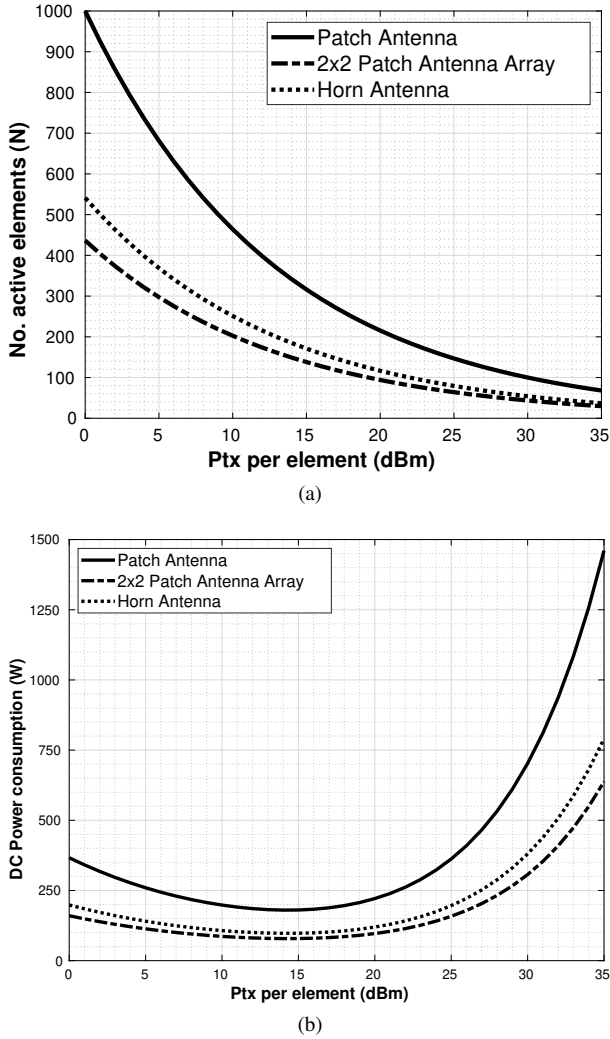
(a)

(b)

Fig. 1. Analytical trade-offs to achieve a given SG using PAAs. Assumptions: $SG = 102$ dBm, $\eta_{PA} = 15\%$, $P_{LNA} = 340$ mW, $P_{TxOH} = P_{RxOH} = 10$ mW. (a) Number of elements computed by using (3). (b) Power consumption computed by using(4).

P_{TxOH} and P_{RxOH}. On the other hand, analyzing Fig. 1 a and b, it can be noted that at the minimum points (regarding power consumption) the corresponding number N_{OP} of active elements required is 342, 149, and 185 respectively. Also, it can be seen that the power consumption increases very gradually, if P_{Tx} per element lies within 14 dBm up to 20 dBm. Therefore, a good tradeoff between power consumption and number of elements (i.e. complexity of the system) is to choose an amplifier with 18 dBm of P_{Tx}, slightly increasing power consumption to 196 W, 86 W, and 106 W, but reducing considerably the number of active elements down to 251, 109, and 136 in the three cases.

A. Beam Steering Capabilities

Starting from the array sizes determined at the end of the previous paragraph, the array pattern was simulated following the three cases by using a square array of:

1) 16×16 patch antenna elements separated half of wavelength. The radiation pattern is represented in Fig. 2a.
2) 11×11 subarrays, where each subarray contains 2×2 patch antenna elements, therefore the separation between sub arrays is one wavelength. The radiation pattern is shown on Fig. 2b.
3) 12×12 horns antennas separated 1.05 wavelength due to the horn size. The radiation pattern is plotted in Fig. 2c.
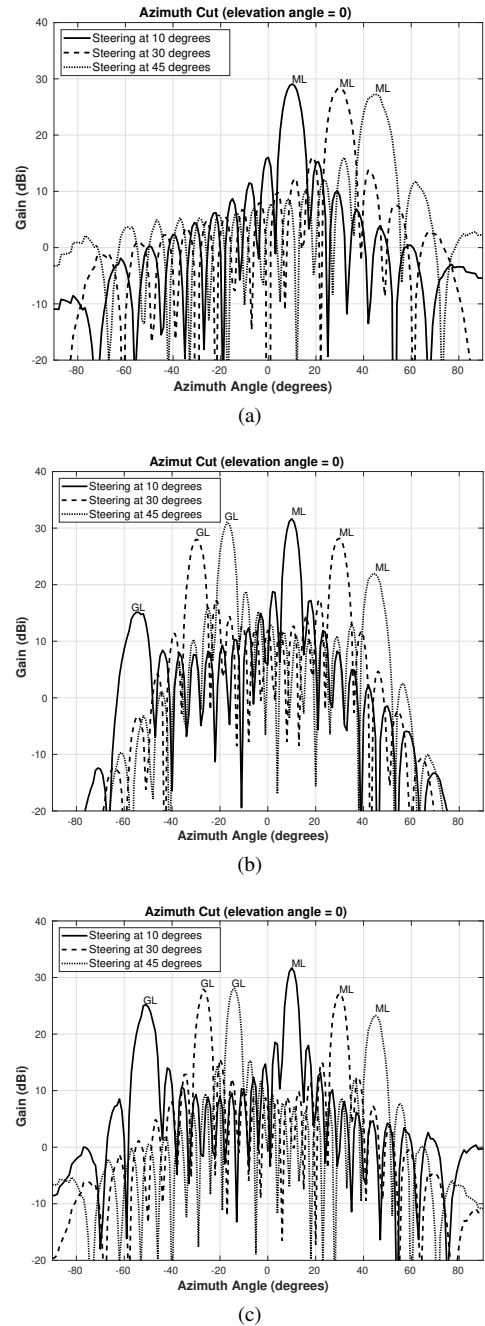

(a)

(b)

(c)

Fig. 2. Steering capabilities for the three cases: (a) 16x16 patch antennas, (b) 11x11 subarrays of 2x2 patch antennas, (c) 12x12 horn antennas.

The results confirm the initial expectations: for case 1, since

114

there is control over every radiating element and the separation is half of the wavelength, the beam steering can be performed without any grating lobes appearing.

On the contrary, in case 2 there is no control over every radiating element and therefore grating lobes begin to appear when beam steering is actuated. For example, when the main lobe (ML) is directed at $10°$, a GL appears at $-57°$ with 16 dB less than the ML, and when the beam is steered at $30°$ the GL appears at $-30°$ with same level as the ML.

On the other hand, the characteristics of beam steering of case 3 are similar to those of case 2, since the distance between the active elements with phase control are similar.

It is important to note that grating lobes are an undesirable phenomenon, even if the system supports working with them, the scan loss is higher when they appear. Taking as a reference the minimum scan angle required $30°$, the scan loss at this angle for the 3 cases are 0.7 dB, 4 dB, 4 dB approximately. Since the SG has to be maintained even when beam steering is applied, the scan loss can be compensated in two ways:

1) by increasing P_{Tx} to 18.7 dBm, 22 dBm, 22 dBm, therefore the power consumption increases to 218 W, 172 W, and 203 W respectively (using (3) and (4));

2) by keeping the same P_{Tx}, but increasing the array size to 280, 203, 252, therefore, increasing the power consumption to 218 W, 158 W, and 196 W respectively.

B. Radiation Masks

For simplicity, the analysis of radiation masks is carried out on the case where grating lobes do not appear, i.e. case 1.

The simulated results prove that square arrays with uniform illumination are not able to comply with ETSI classes 3 and 4. However it is possible to taper the radiation pattern by using non-uniform illumination. Figure 3a shows the radiation pattern of the 16×16 array of patch elements described in case 1, but using a Taylor function for tapering at 16 dB of side lobe level along $\phi = 0$ and $\phi = 90°$. However, this improvement in the radiation pattern comes at a price, i.e. losses of 0.36 dB because of lower illumination efficiency and -3 dB of losses because the array is radiating overall less power.

On the other hand, Fig. 3b shows the radiation pattern of a circularly shaped array with uniform illumination, with the same 256 patch antenna elements. It can be seen that the RPE mask is fulfilled up to ETSI class 3, even without any kind of tapering, it means without any loss of power or efficiency.

As mentioned, the grating lobes are an undesired secondary effect which mainly lead to overstepping the ETSI masks and make unfeasible the practical usage of such radiators. It is also a common practice, even in a single feed parabolic antenna where gratings are not even present, to add an absorptive shroud which is a metallic corona placed around the main dish, which is internally covered by absorptive material. The depth of such external corona is related to the proximity of the unwanted secondary lobe with respect to the main lobe (angularly speaking). In the PAA topology aforementioned, the grating lobes appear far away from the main lobe and thus
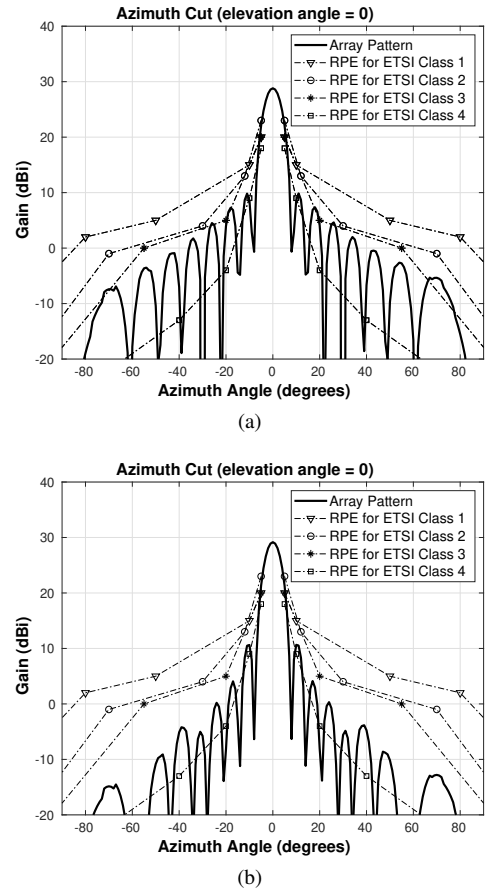

Fig. 3. Array patterns for the case 1. Array size : $M = N = 256$. Antenna element: patch antenna. Inter-antenna distance: $\lambda/2$. (a) 16x16 patch antennas, square shaped array, Taylor illumination, 16dB side lobe level. (b) 256 patch antennas, circular shaped array, uniform illumination.

require a thin shroud, which is practically accepted in a real deployment for preserving the ETSI antenna classification.

V. DISCUSSION

The power consumption of the case 1 (patch base element) and case 3 (horn base element) are similar. However, because of the better beam steering capabilities of the first case as shown in Fig. 2, the third can be discarded.

Case 1 has also a better performance of beam steering than case 2 (base element is a 2x2 patch array), but case 2 consumes less power than case 1. For a better comparison of both cases, let us expand the analysis previously done of scan loss, now considering 2-D beam steering.

Figure 4 shows the scan loss of the cases 1 (a) and 2 (b) for beam steering from $0°$ to $30°$ in 2D. To guarantee the SG even when beam steering is carried out up to $30°$ in azimuth and elevation, 1.5 and 6.3 dB must be compensated for cases 1 and 2. It implies increasing the array size to 18×18 and 17×17, consuming around 252 W and 225 W respectively. Under this constraint the best option is the configuration of case 1, where each the elements is fed by one active component. This is because of the better steering performance and same power consumption compared to case 2.
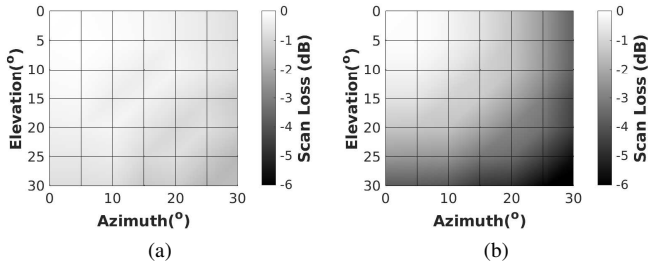
115

Fig. 4. 2D Scan Loss up to 30° for: (a) 16x16 patch antennas and (b) 11x11 subarrays of 2x2 patchs. For a better presentation the scale of (b) is limited to -6dB, however the minimum value is -6.3 dB.

Regarding the compliance of the RPE, a circularly shaped array is definitively the choice for the design, due to its intrinsic capability of tapering the radiation pattern even with uniform illumination as it was shown in Fig. 3b.

FDD Implications

Most wireless-backhaul equipments use frequency-division duplexing (FDD) for transporting bidirectional data streams. Therefore, a duplexer is required to connect the Tx and Rx chains to the antenna. However, getting enough isolation (i.e. 65 dB from SIAE's equipment specification) in the PAA architecture is very difficult due to the available space (i.e. in the order of λ). At this time, the architecture that seems most viable is to have separate antenna arrays for the transmitter and receiver, as it can be seen on Fig. 5. By performing full wave simulations of two arrays at different distances, a reasonable distance of 10 cm guarantees a natural isolation of around 45 dB; therefore, 20 dB are missing to comply with current equipment specifications. As a consequence, a low order filter is required just before the antenna in both the transmitter and the receiver. Since a filter implies an additional loss in the Tx/Rx chain, it will have to be compensated by increasing the array size to preserve the required SG.

VI. CONCLUSIONS

Achieving an acceptable DC power consumption is one of the main challenges when a PAA is going to be used in a commercial wireless backhaul equipment. This is mainly due to the high SG, in turn demanded by the high availability for medium distances to be covered in modern telecom networks.

The minimum power consumption P_{DCmin} achievable given a SG and its corresponding optimum output power P_{TxOP} and number of elements N_{OP} were analytically computed.

Devising a PA whose P_{Tx} is slightly higher than P_{TxOP} is a good trade off between complexity of the PAA ($N << N_{\text{OP}}$) and overall P_{DC} (slightly greater than P_{DCmin}).

Although when a patch antenna is used as the base element (i.e. case 1), the power consumption appears to be greater than when using subarrays of patches (i.e. case 2) or an antenna with more gain (i.e. horn, case 3) as the base element, when it is taken into account that the losses due to beam steering (i.e. scan loss) must be compensated, the energy consumption is
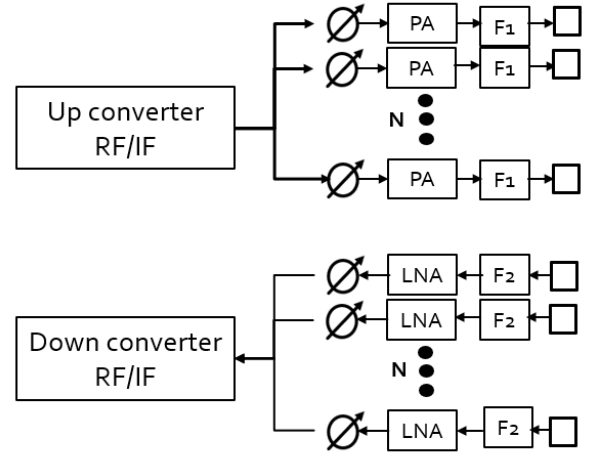

Fig. 5. Architecture for PAA in backhaul equipment. FDD approach.

almost the same for the 3 cases. Therefore the most reasonable choice is case 1, where each patch antenna is fed by an active component and with a very good beam steering performance.

The RPE mask can be fulfilled by using a circularly shaped array. This option is better than using tapering techniques (non uniform illumination of the array), since the fulfillment of the mask is done without any losses or power reduction.

REFERENCES

[1] K. Kibaroglu, M. Sayginer, T. Phelps, and G. M. Rebeiz, "A 64-element 28-ghz phased-array transceiver with 52-dbm eirp and 8–12-gb/s 5g link at 300 meters without any calibration," *IEEE Transactions on Microwave Theory and Techniques*, vol. 66, no. 12, pp. 5796–5811, Dec 2018.

[2] B. Sadhu and et al, "A 28-ghz 32-element trx phased-array ic with concurrent dual-polarized operation and orthogonal phase and gain control for 5g communications," *IEEE Journal of Solid-State Circuits*, vol. 52, no. 12, pp. 3373–3391, Dec 2017.

[3] I. Syrytsin, S. Zhang, G. F. Pedersen, and A. S. Morris, "Compact quad-mode planar phased array with wideband for 5g mobile terminals," *IEEE Transactions on Antennas and Propagation*, vol. 66, no. 9, pp. 4648–4657, Sep. 2018.

[4] W. Hong, Seung-Tae Ko, Y. Lee, and K. Baek, "Compact 28 ghz antenna array with full polarization flexibility under yaw, pitch, roll motions," in *2015 9th European Conference on Antennas and Propagation (EuCAP)*, April 2015, pp. 1–3.

[5] P. Goel and K. J. Vinoy, "A low-cost phased array antenna integrated with phase shifters cofabricated on the laminate," *Progress In Electromagnetics Research B*, vol. 30, pp. 255–277, 2011.

[6] K. Kibaroglu, M. Sayginer, and G. M. Rebeiz, "A low-cost scalable 32-element 28-ghz phased array transceiver for 5g communication links based on a 2×2 beamformer flip-chip unit cell," *IEEE Journal of Solid-State Circuits*, vol. 53, no. 5, pp. 1260–1274, May 2018.

[7] E. T. S. Institute, "Etsi 302 217-4 v2.1.1 : Fixed radio systems; characteristics and requirements for point-to-point equipment and antennas; part 4: Antennas," May 2017.

[8] L. Kong, "Energy-efficient 60ghz phased-array design for multi-gb/s communication systems," Ph.D. dissertation, EECS Department, University of California, Berkeley, Dec 2014. [Online]. Available: http://www2.eecs.berkeley.edu/Pubs/TechRpts/2014/EECS-2014-191.html

[9] S. Caicedo, M. Oldoni, and S. Moscato, "Challenges of using phased array antennas in a commercial backhaul equipment at 26 ghz," in *2019 13th International Conference on Interactive Mobile Communication, Technologies and Learning (5G Fi-Wi for MC Session)*, November 2019.